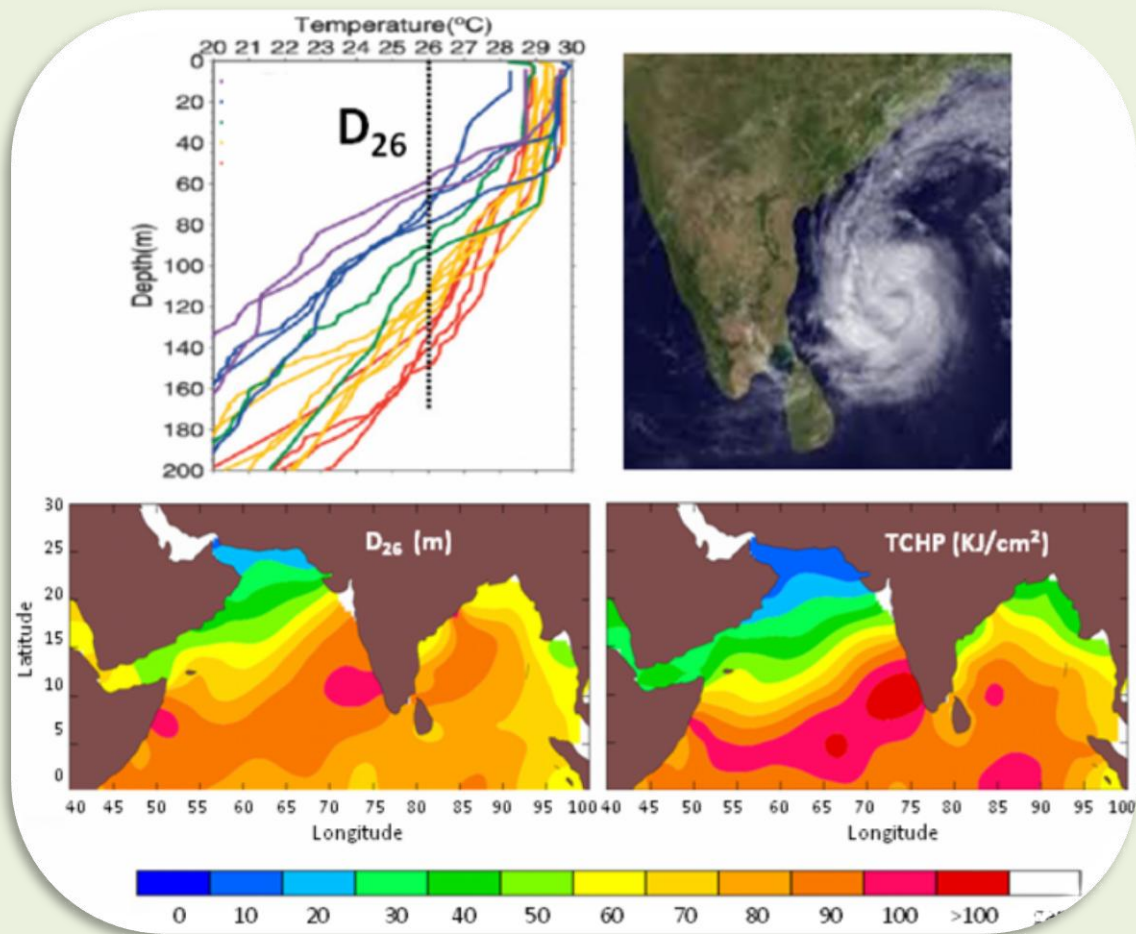


# PREDICTION OF DEPTH OF 26 °C ISOTHERM AND TROPICAL CYCLONE HEAT POTENTIAL USING A ONE-DIMENSIONAL OCEAN MODEL

Ver. 1.0



*nrsc*

Ocean Sciences Group  
Earth and Climate Science Area  
**NATIONAL REMOTE SENSING CENTRE**  
Hyderabad, INDIA

May 2013

**Prediction of Depth of 26 °C Isotherm and Tropical Cyclone Heat Potential  
using a  
One-Dimensional Ocean Model**

ver 1.0

D. Swain

Ocean Sciences Group (ECSA), National Remote Sensing Centre  
Indian Space Research Organisation  
Hyderabad

and

V. C. Navaneeth Krishnan  
Cochin University of Science & Technology, Kochi

**NATIONAL REMOTE SENSING CENTRE  
REPORT/DOCUMENT CONTROL SHEET**

1.	<b>Security Classification</b>	Unclassified		
2.	<b>Distribution</b>	Through soft and hard copies		
3.	<b>Report / Document version</b>	(a) Issue no.: 01	(b) Revision & Date	R01/ May 2013
4.	<b>Report / Document Type</b>	Technical Report		
5.	<b>Document Control Number</b>	NRSC-ECSA-OSG-May2013-TR-529		
6.	<b>Title</b>	Prediction of Depth of 26 °C Isotherm and Tropical Cyclone Heat Potential using a One-Dimensional Ocean Model		
7.	<b>Particulars of collation</b>	<b>Pages:</b> 24	<b>Figures:</b> 11	<b>Tables:</b> 3 <b>References:</b> 48
8.	<b>Author(s)</b>	D. Swain* and V. C. Navaneeth Krishnan <sup>#</sup>		
9.	<b>Affiliation of authors</b>	*Ocean Sciences Group (ECSA), National Remote Sensing Centre, ISRO, Hyderabad  <sup>#</sup> Cochin University of Science & Technology, Kochi		
10.	<b>Scrutiny mechanism</b>	Compiled by: Dr. D. Swain (OSG)	Reviewed by: GH (OSG)	Approved /Controlled by: DD (ECSA)
11.	<b>Originating unit</b>	Ocean Sciences Group, Earth & Climate Science Area, NRSC		
12.	<b>Sponsor(s)/Name and Address</b>	National Remote Sensing Centre, ISRO, Balanagar, Hyderabad-500037		
13.	<b>Date of Initiation</b>	January, 2013		
14.	<b>Date of Publication</b>	May, 2013		
15.	<p><b>Abstract:</b> Oceans play an important role in global climate change as well as several weather phenomena. Two important ocean parameters, the depth of 26 °C isotherm (<math>D_{26}</math>) in the ocean as well as the Tropical Cyclone Heat Potential (TCHP) are responsible for genesis, intensification and propagation of tropical cyclones. Consequently, monitoring of these two parameters and the ability for their advance prediction is quite significant. The present work utilizes a modified one-dimensional (1-D) ocean mixed layer model to predict <math>D_{26}</math> and TCHP 48 hours in advance at an interval of every six hours. The model is forced with forecast surface meteorological parameters obtained from an Atmospheric General Circulation Model. The model results are then validated by comparison with <math>D_{26}</math> and TCHP computed from Argo temperature and salinity profiles for about four months representing the four major seasons in the Indian subcontinent for a one year period. Further, the entire process has been integrated as a single package and automated for operational use.</p> <p><b>Key Words:</b> <math>D_{26}</math>, TCHP, Tropical Cyclones, 1-D model</p>			

# CONTENTS

## Document Control Sheet

<b>Contents</b>	<b>i</b>
<b>Summary</b>	<b>ii</b>
<b>1. Introduction</b> .....	<b>1</b>
1.1. Estimation of $D_{26}$ and TCHP .....	1
1.2. Study Area .....	2
<b>2. Data and Methodology</b> .....	<b>3</b>
2.1. Data .....	3
2.1.1. Argo T/S profiles .....	3
2.1.2. Data for 1-D ocean model .....	4
2.2. Methodology .....	4
<b>3. Validation of Model Predictions</b> .....	<b>6</b>
3.1. Validation of Model Predicted $D_{26}$ .....	7
3.2. Validation of Model Predicted TCHP .....	10
<b>4. Spatial Variability of Model Predicted <math>D_{26}</math> and TCHP</b> .....	<b>12</b>
<b>5. Conclusions</b> .....	<b>15</b>
<b>Acknowledgements</b> .....	<b>16</b>
<b>References</b> .....	<b>17</b>
<b>Appendix – I: Package Execution Environment</b> .....	<b>21</b>
<b>Appendix – II: Locations of ARGO floats used for validation of model results</b> .....	<b>22</b>

## Summary

Oceans play an important role in global climate change. Coupled with the atmosphere, they are responsible for formation, sustenance as well as termination of several weather and climate phenomena. In this context, the depth of 26 °C isotherm ( $D_{26}$ ) in the ocean as well as the Tropical Cyclone Heat Potential (TCHP) are two important ocean parameters responsible for genesis, intensification and propagation of tropical cyclones. Consequently, monitoring of these two parameters and the ability for their advance prediction is quite significant. In the present work, a one-dimensional (1-D) ocean mixed layer model has been suitably modified to predict  $D_{26}$  and TCHP 48 hours in advance at an interval of every six hours. Required algorithms for the estimation of  $D_{26}$  and TCHP have been developed and integrated into the model domain. The model is forced with forecast surface meteorological parameters obtained from an Atmospheric General Circulation Model. Model results are then validated by comparison with  $D_{26}$  and TCHP computed from Argo temperature and salinity profiles for about four months during the year 2012, representing the four major seasons in the Indian subcontinent. The validation results and spatio-temporal variability of the two parameters are presented and analyzed for the North Indian Ocean on the basis of model predictions. The overall correlation coefficient [Root Mean Square error: RMSE] between model and Argo estimated  $D_{26}$  is 0.88 [9.54 m] for 12-hour and 0.89 [9.89 m] for 48-hour predictions, respectively. Similarly, the overall correlation coefficient [RMSE] between model and Argo estimated TCHP is 0.92 [12.17 KJ/cm<sup>2</sup>] for 12-hour and 0.92 [11.77 KJ/cm<sup>2</sup>] for 48-hour predictions, respectively. From the analysis of the spatio-temporal variability of  $D_{26}$  and TCHP in the North Indian Ocean, it is observed that they largely follow the seasonal dynamics and thermodynamics of the region as well as the regional large and small scale ocean-atmospheric features prevalent in the region. The entire process of data processing, model run and visualization is further integrated into a single package and automated using open source softwares, which could be deployed for operational use.

## 1. Introduction

Over the years, the oceans have been recognized as one of the major contributors to climate change, in part owing to their large thermal inertia. Being the largest solar energy collector, they store huge amounts of heat energy within the upper few layers on shorter time scales and in the deeper layers on longer time periods. The upper layer, usually known as ocean's troposphere is regarded as the most active part of the ocean because of the heat flux exchange between atmosphere and the ocean [Momin *et al.*, 2011]. The ocean heat content (OHC) in the upper layers is thus important for understanding the role of air-sea interaction process and its contribution to global climate [Hastenrath *et al.*, 1980].

Tropical Cyclones (TCs) are one of the outcome of this air-sea interaction and they considerably affect many physical parameters of the ocean. Also, passage of TCs over warm oceanic features may intensify them or change its track [Shay *et al.*, 2000]. Tropical Cyclone Heat Potential (TCHP) is a parameter describing OHC which is available for cyclone formation and intensification changes [Wada and Usui, 2007; Wada and Chan, 2008; Ali *et al.*, 2004, 2007; De Maria *et al.*, 1994, 2005, 2009]. TCHP is defined as a measure of the integrated vertical temperature from the sea surface to the depth of the 26 °C ( $D_{26}$ ) isotherm [Goni *et al.*, 2003, 2009]. Given the above background, monitoring of the upper ocean thermal structure has attained importance in the study of cyclone-ocean interaction with respect to the prediction of TC intensity and tracks, and hence the predictive value of parameters like  $D_{26}$  and TCHP.

### 1.1. Estimation of $D_{26}$ and TCHP

$D_{26}$  (in m), is estimated from *in situ* temperature profiles of ocean which are collected using CTDs/XBTs/XCTDs. This is usually done by scanning the temperature profile from the surface till the depth at which the temperature value is or just decreases below 26 °C. TCHP ( $\text{KJ}/\text{cm}^2$ ) is computed utilizing temperature profiles again using the expression:

$$TCHP = \rho C_p \int_0^{D_{26}} [T(z) - 26] dz \quad (1)$$

where,  $\rho$  is the density of sea water at the surface (assumed constant),  $C_p$  is the specific heat capacity of sea water at constant pressure  $p$ ,  $T$  is the temperature (°C) of each layer of ocean thickness “ $dz$ ” and  $D_{26}$  the depth of the 26 °C isotherm. When, the Sea Surface Temperature (SST) is 26 °C or below 26 °C, TCHP is taken to be 0.

Apart from *in situ* temperature profiles, other methods to estimate TCHP include using a reduced gravity model utilizing the relationship between dynamic height and mass field of the

ocean [Goni *et al.*, 1996], linear regression between the depth of isotherms from 26 °C to 28 °C as obtained from synthetic temperature profiles and the dynamic topography estimated from the altimetry, and isotherm depths obtained from satellite derived Sea Surface Height Anomaly (SSHA) along with climatological temperature profiles to provide synthetic temperature profiles from which TCHP is then estimated [<http://www.aoml.noaa.gov/phod/cyclone/data/method.html>]. The later approaches use  $D_{26}$  values obtained from climatological temperature profiles. Ali *et al.* [2012] have also used the ANN technique to obtain TCHP from satellite derived near real time SSHA, SST, and climatological  $D_{26}$ .

In the present work, an one-dimensional (1-D) ocean model is improvised for obtaining  $D_{26}$  and TCHP values with the primary objective to predict  $D_{26}$  and TCHP.

## 1.2. Study Area

The North Indian Ocean region (NIO: 0° to 30° N and 40° E to 100° E) has been considered as the study area in the present work (Figure 1). The Indian Ocean region is highly complex, least studied and least understood oceanographically comparing with the other world oceans [Swallow *et al.*, 1984]. It is influenced by a semi-annually reversing monsoon thus presenting a wide variety of oceanographic and atmospheric phenomena. The Indian landmass as a result also experiences four primary seasons, namely, winter or northeast monsoon (December – February), summer or pre-summer monsoon (March – May), the southwest or summer monsoon season (June – September) and a post-summer monsoon season (October & November). NIO can be broadly divided in to the Arabian Sea (AS, 5° N to 30° N and 40° E to 76° E) and the Bay of Bengal (BoB, 5° N to 30° N and 76° E to 100° E longitude). The various oceanographic and atmospheric features of the NIO have been discussed in great detail in several earlier works [Düing and Leetmaa, 1980; Bruce, 1983; Potemra *et al.*, 1991; Shankar *et al.*, 1996; Shetye *et al.*, 1996; Varkey *et al.*, 1996; Prasad, 1997; Murtugudde and Busalacchi, 1999].

The NIO and in particular the BoB is an intense cyclone prone area. The devastations caused by the TCs in this region have high economic and humanitarian implications. Land falling of cyclones cause devastating disasters in the countries outlining the NIO because of their large population density and low socio-economic condition [Webster *et al.*, 1998; Belanger *et al.*, 2012].

It is a fact that eight of the ten deadliest TC's of all time have occurred in Bay of Bengal and Arabian Sea with five making impact in Bangladesh and three making landfall in India

[WMO/TD No. 84, 2011]. This necessitates the advanced forecasting of TCs in terms of cyclogenesis, propagation tracks, intensities and probable landfall points in this region thus demanding information/predictions of  $D_{26}$  and TCHP variability in the NIO.

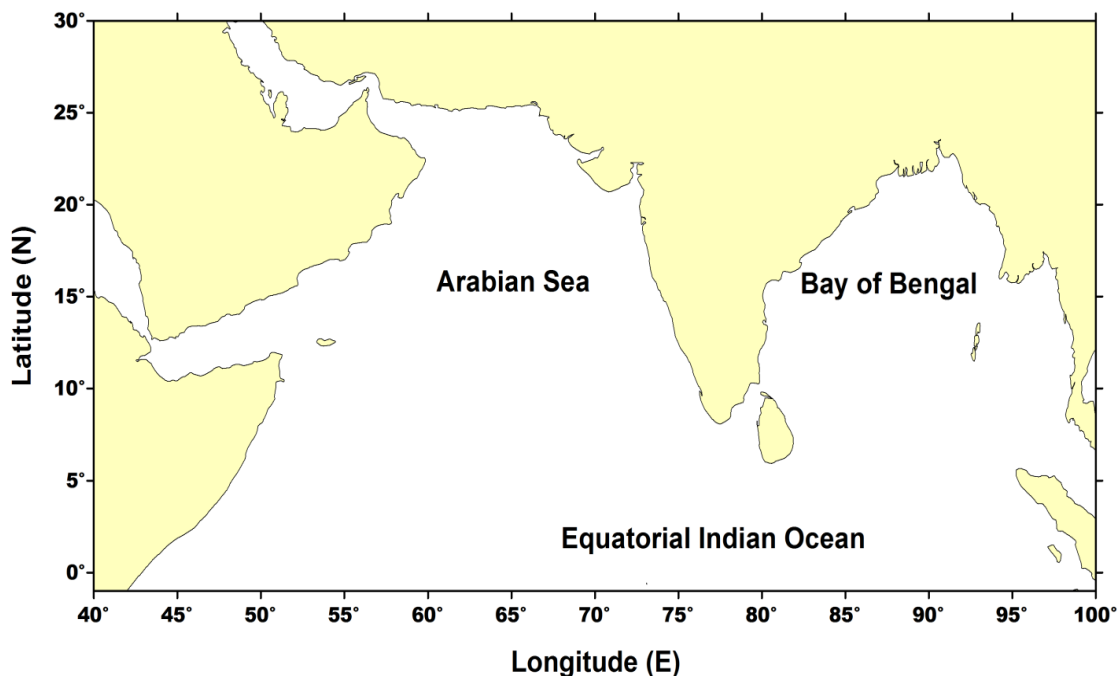


**Figure 1: Schematic of the Study Area: The North Indian Ocean**

## **2. Data and Methodology**

In the present work, the 1-D Price-Weller-Pinkel [*Price et al.*, 1986] ocean mixed layer model has been improvised for obtaining  $D_{26}$  and TCHP. The algorithms for estimating  $D_{26}$  and TCHP have been developed using *in situ* temperature and salinity (T/S) profiles from Argo floats. The same are then integrated into the model and model estimated results are validated by comparison with  $D_{26}$  and TCHP estimated from Argo T/S profiles. The data used for running the model as well as for the validation purpose are briefly described below.

### **2.1. Data**

The primary data used in the present work for validation of the model simulated  $D_{26}$  and TCHP computation are ocean depth and T/S profiles. They have been collected from the Argo program.

#### **2.1.1. Argo T/S profiles**

Quality controlled Argo T/S profiles have been collected from the Argo program made freely available through INCOIS through their web-portal [[http://www.incois.gov.in/Incois/argo/argo\\_Regional\\_Centre.jsp](http://www.incois.gov.in/Incois/argo/argo_Regional_Centre.jsp)]. Argo is an ocean observation

system for the earth's oceans that provides real time data which can be used in climate, weather, oceanography and fishery studies. Argo consists of a collection of small drifting buoys deployed all over the world. They descend down the ocean up to a depth of ~ 2 Km and measure conductivity and temperature profiles while coming up. After reaching the surface, the data are transmitted to the on-shore centers via satellites. The vertical resolution of the T/S profiles data is ~ 10 m in the upper layers of the ocean.

### **2.1.2. Data for 1-D ocean model**

The data needed for running the modified Price-Weller-Pinkel (PWP) model are climatology T/S profile with surface meteorological forcings of climatological peak radiation (PR) of the day, net heat loss (NHL) from the ocean, and surface wind speed (WS).

Monthly climatological T/S profiles from The World Ocean Atlas 2005 (WOA05) database [Locarnini *et al.*, 2006; Antonov *et al.*, 2006] have been used in the current work regridded at 0.5 X 0.5 spatial resolutions at each depth level. The T/S profiles have been linearly interpolated in to 1m resolution up to 250 m from the surface in the PWP model internally. These modified profiles are used for the model initialization.

PR climatology obtained from the Comprehensive Ocean-Atmosphere Data Sets (COADS) at 0.5° X 0.5° grid has been used. SW and NHL 6 hourly forecast fields for 48 hours duration have been obtained from an Atmospheric General Circulation Model (T574) run at from National Centre for Medium Range Weather Forecasting (NCMRWF). These forecasts are generated at 0.5 X 0.5 spatial grids globally on a daily basis by running the T574 model.

Further, Global 2-Minute Gridded Elevation Data, version 2 [ETOPO2v2, 2006] data obtained from National Geophysical Data Center (NGDC) is provided to the model as an input to prevent the model from over estimation of parameters. Further details on the model data and parameters may be found in Swain & Ali [2011].

## **2.2. Methodology**

In the present work, Argo T/S and depth profiles have been used for formulating and validating the TCHP and  $D_{26}$  computation algorithm. TCHP which is also a measure of energy available for cyclones is computed by summing the heat content in a column of water where SST is above 26°C using equation (1). When SST is below 26 °C, TCHP for the layer is assumed to be zero.  $D_{26}$  is expressed in m and TCHP in  $\text{KJ}/\text{cm}^2$ . It is also to be noted that density of the sea water

" $\rho$ " is not taken to be a constant, but calculated at each layer from the T/S values based on the United Nations Educational, Scientific, and Cultural Organization (UNESCO) equation for density [Millero and Poisson, 1981].

For  $D_{26}$  and TCHP predictions, the 1-D PWP model as used by Swain and Ali [2011] is further modified. The model was originally used for Mixed Layer Depth (MLD) estimation [Price et al., 1986]. The model provides synthetic T/S profiles as the output based on the ocean surface forcings of NHL, PR, & SW. These T/S profiles along with the depth information are then utilized to obtain  $D_{26}$  and then TCHP by integrating the  $D_{26}$ -TCHP subroutine in to the model code. The PWP model provides an estimation of the desired parameter at a single location only and is run at different locations (grids) based on the desired and available forcing data resolution to simulate distribution of  $D_{26}$  and TCHP. In the present work  $D_{26}$  and TCHP predictions are made at  $0.5^\circ \times 0.5^\circ$  grid resolutions over the NIO. The entire process starting with the data pre-processing to model run and finally graphical visualization have been integrated into a single package and automated. More details on the software requirements for this are provided in Appendix – I. Figure 2 presents a flow-diagram illustration of the entire process.

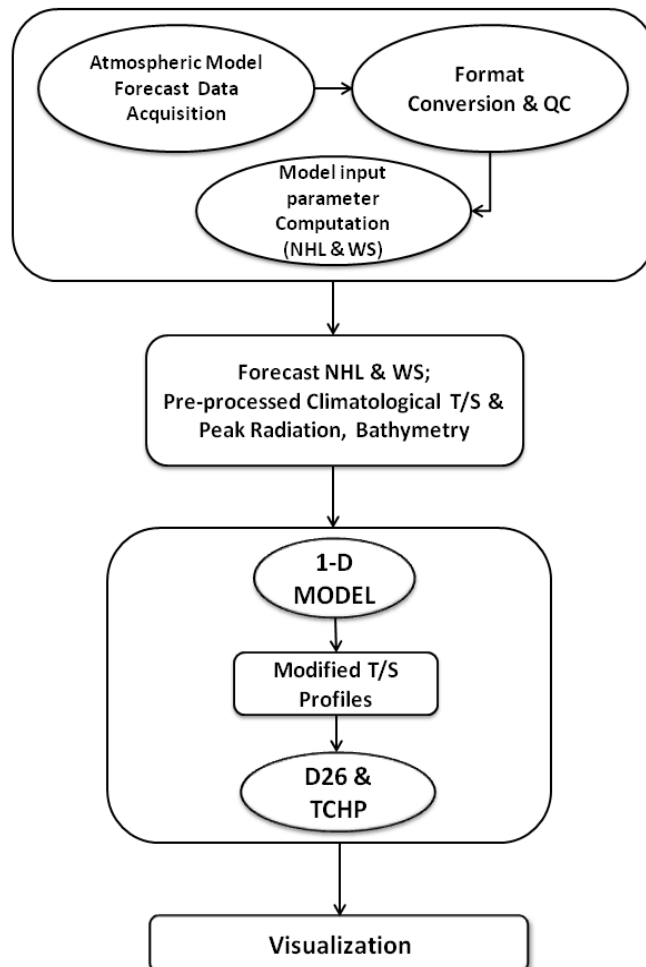


**Figure 2: A flow-diagram illustration of the scheme for prediction of  $D_{26}$  and TCHP**

For validation of the model predicted  $D_{26}$  and TCHP, they are collocated with the available Argo observations. For this, the model grid value nearest to the *in situ* (Argo) location and within a search radius of  $0.5^\circ$  is considered as collocated. If there are multiple nearest values within this search radius, then the average of all the values is considered. Statistical analysis is carried out on the comparisons of model and Argo values and the spatio-temporal variability of the model predicted  $D_{26}$  and TCHP over the NIO is analyzed on the basis of dynamics and thermodynamics of the region.

### 3. Validation of Model Predictions

The modified 1-D PWP model provides predictions of  $D_{26}$  and TCHP based on 6 hourly atmospheric forecasts from T574 made available by NCMRWF. The model predicted values are compared with  $D_{26}$  and TCHP estimated from collocated Argo T/S profiles during 2012. For this, 12 hour model predictions have been considered for same day comparisons and 48 hour predictions with the corresponding day Argo observations. The comparisons are made for months representative of each of the seasons, namely January for winter monsoon, April for summer, July for southwest monsoon and November for post-summer monsoon period. Further, the dates have been chosen randomly according to the availability of Argo data for the representative months and time for Argo is not explicitly considered for collocation as this information is not available for all the profiles.

All the locations over which  $D_{26}$  and TCHP from *in situ* (Argo T/S profiles) and model values have been compared for the four representative months are shown in Figure 3.

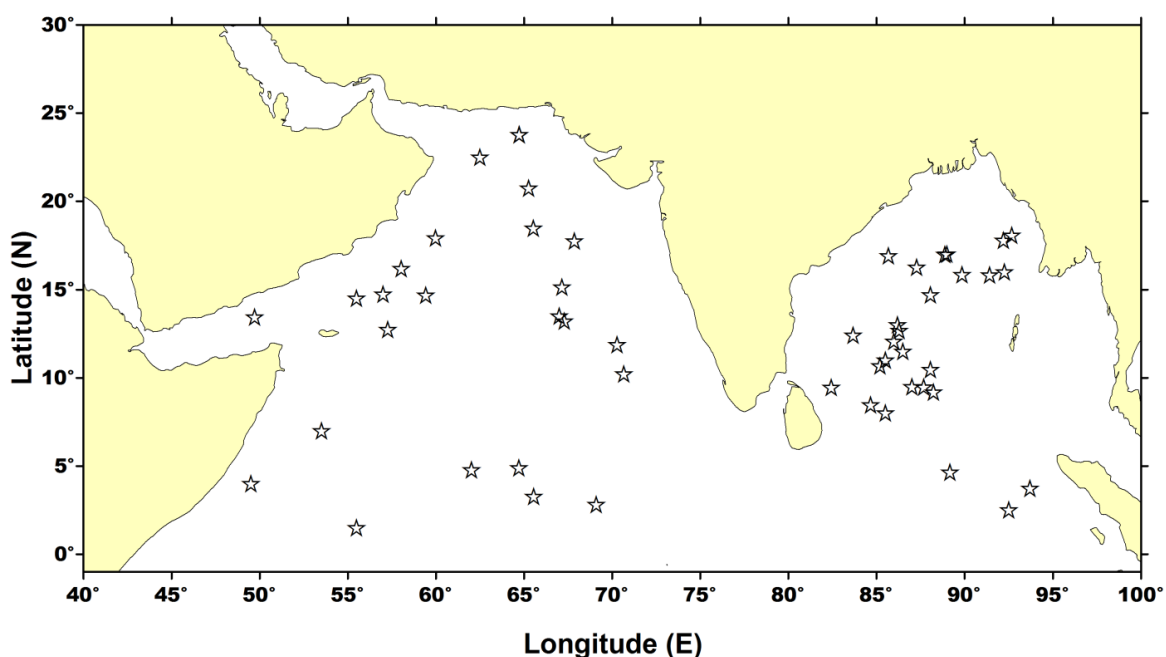


Figure 3: Locations (ARGO floats) of model validation

Table-1 presents the number of collocated Argo observations available for comparison with model values on different dates during 2012 and the corresponding Argo locations provided in Appendix - II.

**Table 1: Details of Available Argo Observations for Model Validation**

Month (2012)	12-hours			48-hours		
	Date	No. of Obs.	Total Obs.	Date	No. of Obs.	Total Obs.
Jan	01	5	20	03	5	20
	15	11		15	11	
	16	2		16	2	
	30	2		30	2	
Apr	01	2	20	03	2	20
	15	9		15	9	
	16	6		16	6	
	30	3		30	3	
Jul	01	5	20	03	5	20
	02	2		04	2	
	09	1		09	1	
	12	2		12	2	
	15	7		15	7	
	16	3		16	3	
Nov	01	2	20	03	2	20
	04	3		04	3	
	15	8		15	8	
	21	2		21	2	
	22	3		22	3	
	25	2		25	2	

### 3.1. Validation of Model Predicted $D_{26}$

The modified 1-D model was used to obtain  $D_{26}$  predictions at 6 hourly intervals for 48 hours and for a one year period. Argo float locations and T/S data were then collected for some of the random dates and  $D_{26}$  was estimated using the algorithm developed earlier. Corresponding collocated values were picked up from the model dates taking care of spatial and temporal collocation conditions as mentioned in section 4.2 and statistical analysis were carried out. Figure 4 presents the overall scatter between collocated model and Argo estimated  $D_{26}$  with the statistical details presented in Table 2. Table 2 also presents the statistical details for comparisons pertaining to individual months which are taken as representative of the seasons with the corresponding scatters for 12-hour and 48-hour predictions presented in Figures 5 & 6, respectively.

**Table 2: Statistical Analysis for the comparison of  $D_{26}$  from model and Argo**

Units: m	12-hour Advance Predictions					48-hour Advance Predictions				
Param.	2012	Jan	Apr	Jul	Nov	2012	Jan	Apr	Jul	Nov
No. of Obs.	80	20	20	20	20	80	20	20	20	20
Std. Dev. Model [Argo]	16.46 [19.31]	14.39 [18.67]	15.22 [20.73]	15.65 [17.88]	19.20 [20.87]	17.87 [20.52]	19.93 [20.81]	16.23 [22.36]	14.80 [17.28]	19.21 [20.99]
Corr. Coeff. (R)	0.88	0.83	0.93	0.94	0.90	0.89	0.88	0.94	0.90	0.90
Slope	0.75	0.64	0.68	0.82	0.83	0.77	0.84	0.68	0.77	0.83
Intercept	13.00	16.98	21.32	10.99	5.09	12.19	4.01	22.78	13.94	5.83
Bias	-2.95	-6.55	1.08	-0.93	-5.41	-3.03	-7.76	1.33	-0.97	-4.71
RMSE	9.54	12.09	8.39	6.27	10.41	9.89	12.58	9.04	7.32	9.90

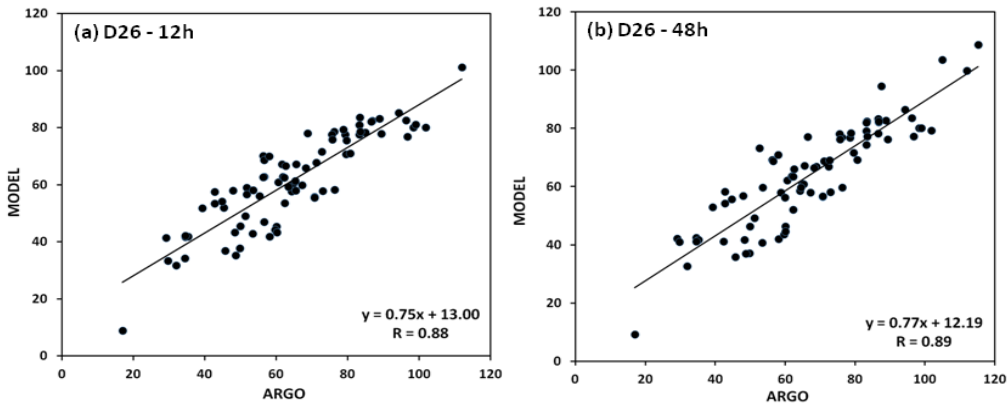


**Figure 4: Overall Scatters between model & Argo estimated  $D_{26}$  (m) for (a) 12-hr & (b) 48-hr**

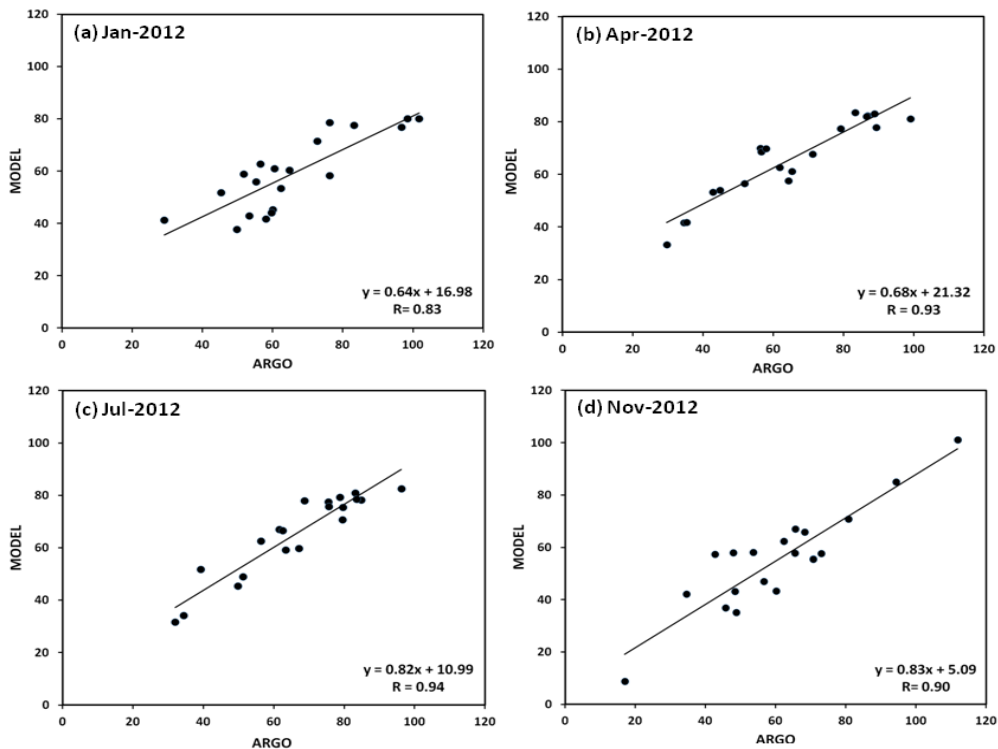


**Figure 5: Scatters between 12-hour model predicted and Argo estimated  $D_{26}$  (in m)**

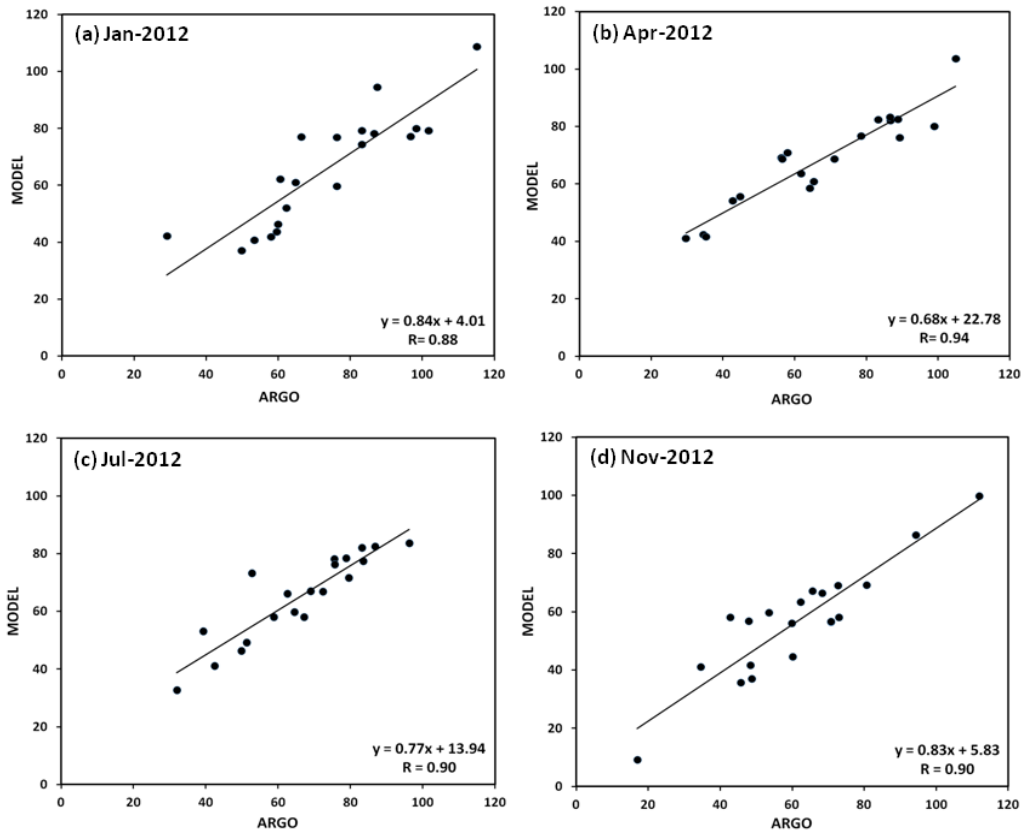


**Figure 6: Scatters between 48-hour model predicted and Argo estimated  $D_{26}$  (in m)**

From the scatters between model predicted  $D_{26}$  and those estimated from Argo profiles, the correlation coefficient (R) is 0.88 (0.89) for 12-hour (48-hour) predictions with corresponding root mean square error (RMSE) of 9.54 m (9.89 m). For individual months representing the winter, summer, summer monsoon and post-summer monsoon periods during 2012, R is greater than 0.90 for 12-hour as well as 48-hour predictions except during January. It is well known that convective mixing due to winter cooling is one of the important mechanisms active in the NIO during this period. Since, the model is forced with PR climatology only and the winds are relatively weak, the model is not able to simulate the vertical thermal structure very accurately as compared to other seasons and hence the lesser R. It may also be noted that the standard deviation (SD) in case of model predictions is lower than those estimated from Argo observations. These points to the larger variation in  $D_{26}$  values obtained from Argo than model which is obvious as all the real time physical processes contributing to the variability of the ocean thermal structure cannot be modeled. Overall, as seen from the comparative table and Figures (4 – 6), the model is able to perform quite satisfactorily in predicting  $D_{26}$  both at 12-hours and 48-hours.

As had been mentioned earlier, though the model predictions are available at every 6-hourly

interval and we have considered only the 12-hour and 48-hour as test cases, it is very likely that the model also performs satisfactorily for other intervals of predictions till 48-hours.

### 3.2. Validation of Model Predicted TCHP

The model predicted TCHP values are validated with the corresponding values computed from the Argo profiles. Table 3 presents the statistical details for comparisons pertaining to individual months as well as overall with the corresponding scatters for 12-hour and 48-hour predictions presented in Figures 7 – 9, respectively.

**Table 3: Statistical Analysis for the comparison of TCHP from model and Argo**

Units: KJ/cm <sup>2</sup>	12-hour Advance Predictions					48-hour Advance Predictions				
Param.	2012	Jan	Apr	Jul	Nov	2012	Jan	Apr	Jul	Nov
No. of Obs.	78	19	20	20	19	78	19	20	20	19
Std. Dev. Model [Argo]	26.21 [25.98]	13.12 [17.71]	28.50 [31.39]	23.04 [22.65]	22.76 [24.23]	25.79 [25.74]	18.68 [20.27]	28.00 [31.39]	21.39 [21.35]	23.03 [25.05]
Corr. Coeff. (R)	0.92	0.89	0.96	0.95	0.85	0.92	0.90	0.96	0.97	0.87
Slope	0.93	0.66	0.87	0.97	0.80	0.92	0.83	0.86	0.97	0.80
Intercept	-2.62	2.30	3.61	2.05	-3.39	-2.27	-2.26	4.53	1.90	-3.65
Bias	-6.19	-9.43	-3.77	0.17	-12.18	-6.02	-9.00	-3.73	0.34	-12.15
RMSE	12.17	12.50	9.35	7.03	17.54	11.77	12.42	9.44	5.13	17.13

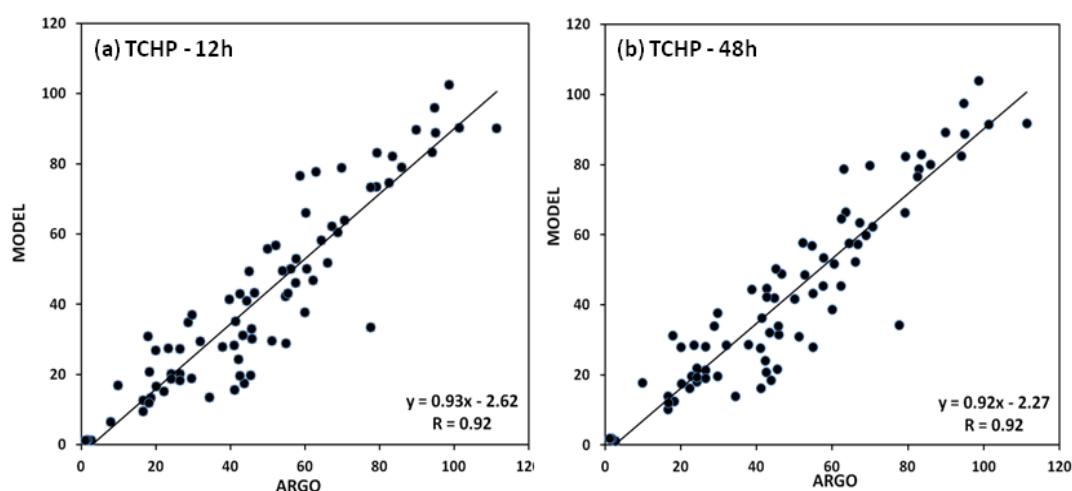


**Figure 7: Overall Scatters between model predicted & Argo computed TCHP (KJ/cm<sup>2</sup>) for (a) 12-hr & (b) 48-hr**

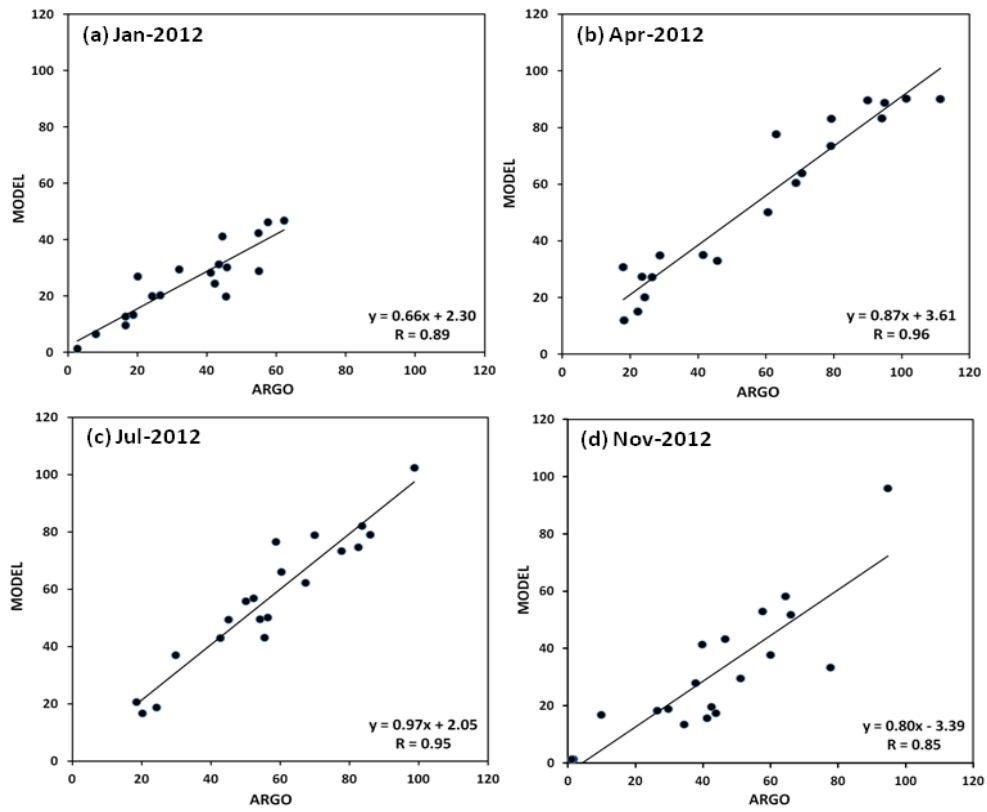


Figure 8: Scatters between 12-hour model predicted & Argo computed TCHP (in KJ/cm<sup>2</sup>)

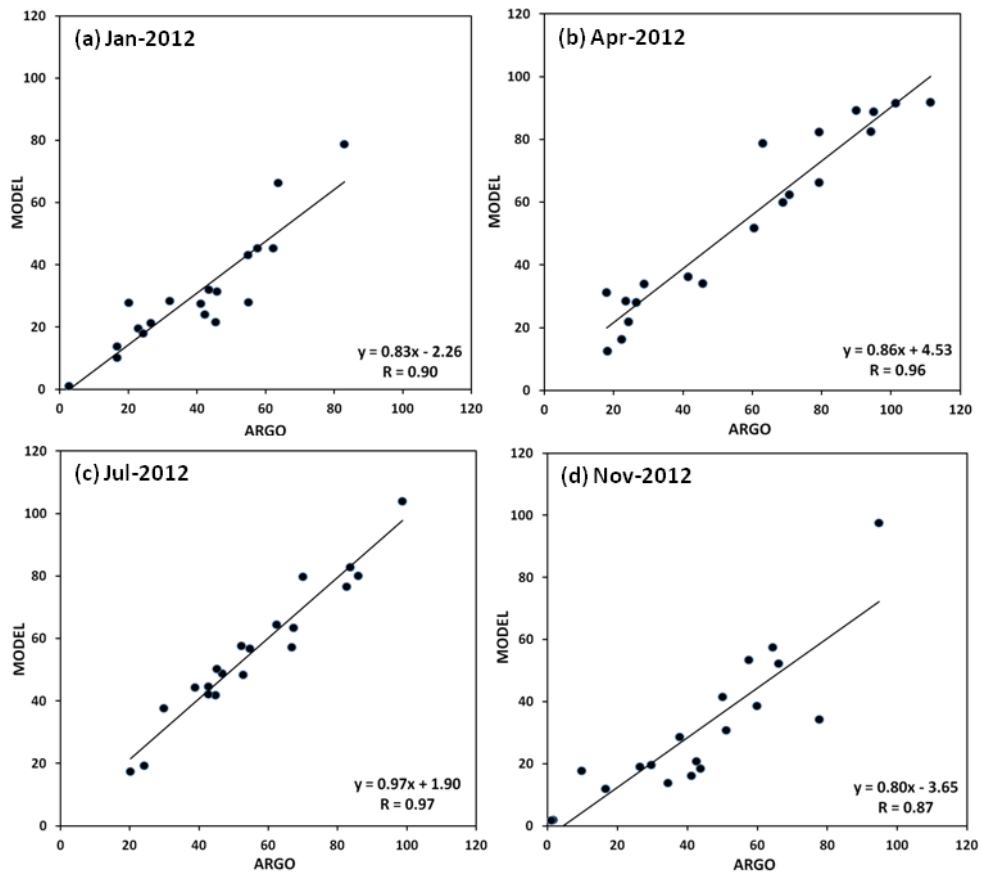


Figure 9: Scatters between 48-hour model predicted & Argo computed TCHP (in KJ/cm<sup>2</sup>)

From the scatters between model predicted TCHP and those computed from Argo profiles (Figure 7), and the statistical analysis presented in Table 3, R is 0.92 (0.92) for 12-hour (48-hour) predictions with corresponding RMSE of 12.17 KJ/cm<sup>2</sup> (11.77 KJ/cm<sup>2</sup>). For individual months representing the winter, summer, summer monsoon and post-summer monsoon periods during 2012, R is greater than 0.85 for 12-hour as well as 48-hour predictions and greater than 0.95 for April and July. Further, in contrast to the observations with D<sub>26</sub>, the SD in case of model predictions is sometimes higher for TCHP than those computed from Argo observations, for example during July and overall for 12-hour as well as 48-hour predictions. As seen from the comparative table and Figures (7 – 9), the model is able to predict TCHP both at 12-hours and 48-hours with reasonable accuracy.

#### **4. Spatial Variability of Model Predicted D<sub>26</sub> and TCHP**

Coloured contours for 12-hour and 48-hour model predictions of D<sub>26</sub> and TCHP for the 15<sup>th</sup> day of the four seasonal representative months have been plotted to visualize the spatial variability of the two parameters over the NIO. Left hand panels of Figure 10 present the 12-hour D<sub>26</sub> predictions and the 48-hour predictions are shown in the right hand panels on the 15<sup>th</sup> day of the four months representing the four seasons, namely winter (north-east monsoon), summer, summer monsoon (south-west) and post-summer monsoon.

The Indian Ocean is a very unique region because of the monsoon reversals, fresh water influx, and insolation. Heat content variability appears to be the outcome of vertical movement of the thermocline which is the result of the ocean's response to the seasonally varying wind and solar insolation [Mowla, 1970; Panchawagh, 2006]. Hence, the major factors contributing to the variability of D<sub>26</sub> and TCHP in the NIO would be in terms of the solar heating, wind stress, and freshwater flux.

During the winter season (December – February), solar heating is low but due to the north westerly winds active during the period, evaporation is high. This causes increase in salinity and cooling of the upper layers of the ocean in general. This increase in salinity causes increase in density which initiates winter convection [Babu et al., 2008; Hacker et al., 1998; Kumar and Prasad., 1996], which could result in decrease in D<sub>26</sub> in the north western AS (data not available in the figure presented) with higher values in the south central AS (Figure 10-L1 & R1). In BoB, during the summer monsoon, there is large freshwater intrusion resulting in low salinity with surface stratification [Kumar and Narvekar, 2005, 2006; Mohan and Gupta, 2011]. As a consequence, even the winter cooling of the surface in the succeeding seasons cannot initiate

convective mixing in BoB.  $D_{26}$  is thus shallow in the north and slightly deeper in the south. During spring inter monsoon season (March – May), solar heating is at its maximum and the winds are weaker in the entire NIO.  $D_{26}$  is thus deeper during this time in the AS as is also seen from the figures (Figure 10 – L2 & R2). However, in BoB conditions similar to the winter prevails even during this season. Though insolation is high, because of the adequate fresh water influx surface will be stratified resulting in shallow  $D_{26}$  in the north BoB but with slightly deeper values in the southern BoB.

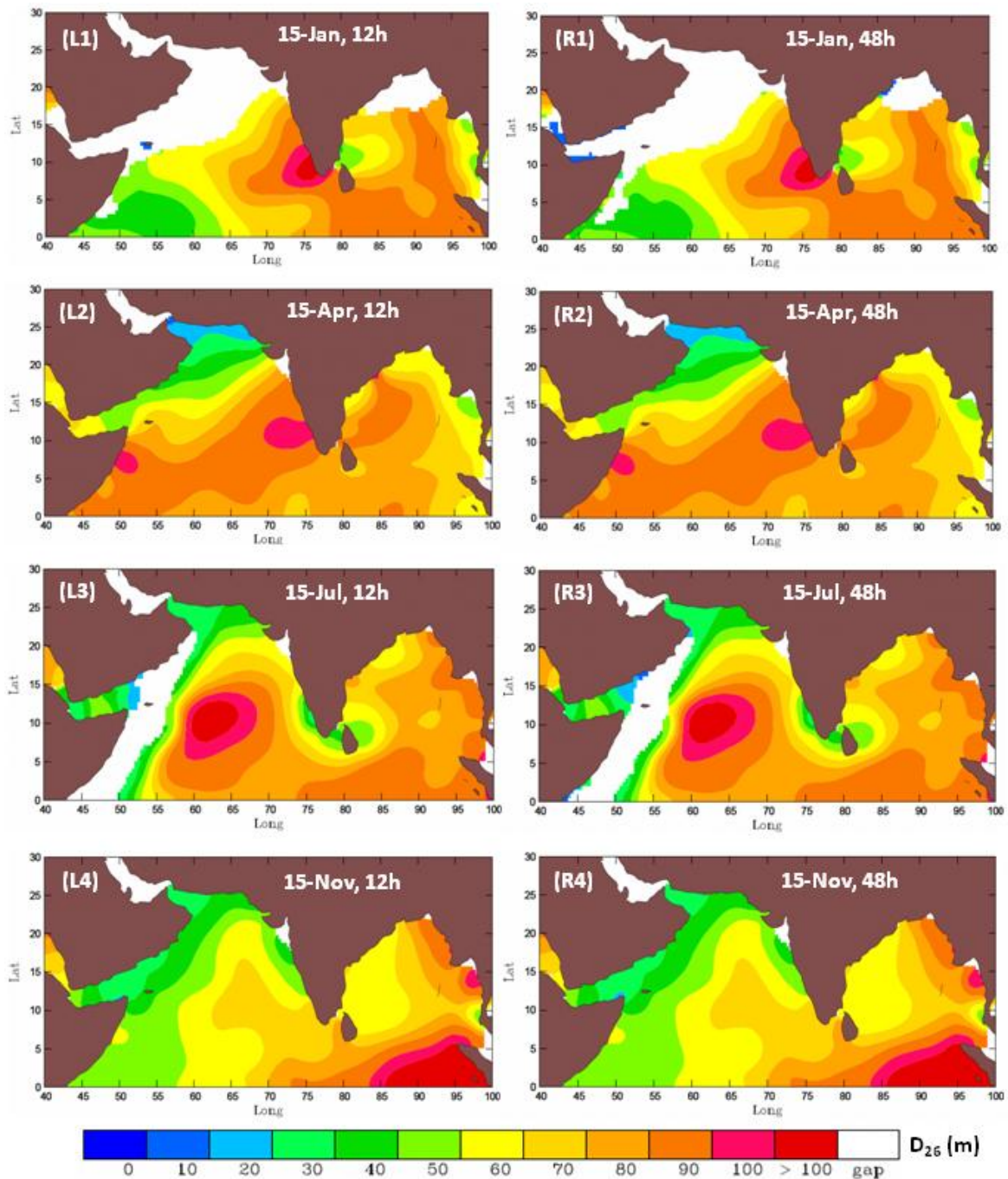


**Figure 10: Spatial Variability of Model Predictions of  $D_{26}$  on 15<sup>th</sup> day for 4 months during 2012 (L1-L4: 12-h predictions; R1-R4: 48-h predictions)**

The summer monsoon or the southwest monsoon (June-September) in the NIO is marked by strong winds resulting in mixing of the surface mixed layers. The  $D_{26}$  values are greater than 80 m almost throughout the basin (Figure 10-L3 & R3) with highest values in the central AS. The inter-monsoon period of October-November experiences low wind speed over most parts of the NIO coupled with low NHL by the ocean and moderate PR. Consequently  $D_{26}$  is relatively shallow (less than 60 m) in most parts of the NIO (Figure 10 – L4 & R4).

The 12-hour and 48-hour model predictions for TCHP are shown in the left hand and right hand panels of Figure 11, respectively for the period as mentioned earlier for  $D_{26}$ . TCHP which is computed considering the SST and  $D_{26}$  follows the spatial variability as exhibited by  $D_{26}$  generally. The patterns are almost similar to that of variability in  $D_{26}$ , however with different magnitudes. TCHP ranges from a minimum of  $\sim 10$  KJ/cm<sup>2</sup> in most parts of the NIO during the winter monsoon period (Figure 11 – L1 & R1) and post-summer monsoon period (Figure 11 – L4 & R4) to as high as 100 KJ/cm<sup>2</sup> or more during the pre-summer monsoon period represented by the month of April (Figure 11 – L2 & R2).

When the southwest monsoon starts, solar heating decreases and wind stress increases. The high precipitation over the Indian Ocean reduces the heat content resulting in shallow  $D_{26}$  and thereby low TCHP in the AS. Intense upwelling zones appear in the western and eastern parts of the AS resulting in shallow  $D_{26}$  [Vinayachandran and Shetye, 1991; Vinayachandran, 2004; Takeshi et al., 2008]. Upwelling is very prominent near the coast of Africa especially off the Somali coast [Rao et al., 1992, Muraleedharan and Kumar, 1996, Suryanarayana et al., 1992]. These zones thus experience lower TCHP values. The summer monsoon period in general experiences intermediate values of TCHP ranging between 60 – 90 KJ/cm<sup>2</sup> over most parts of the NIO (Figure 11 – L3 & R3).

The fall inter monsoon season brings with it increase in insolation, reduced wind speed, and increased SST, therefore increasing  $D_{26}$  slightly and TCHP in the central and south AS [Vinayachandran and Shetye, 1991; Jaswal et al., 2012].

The contours plots presented above are also the sample plots that are the final outcome after running of the entire package developed for the purpose.

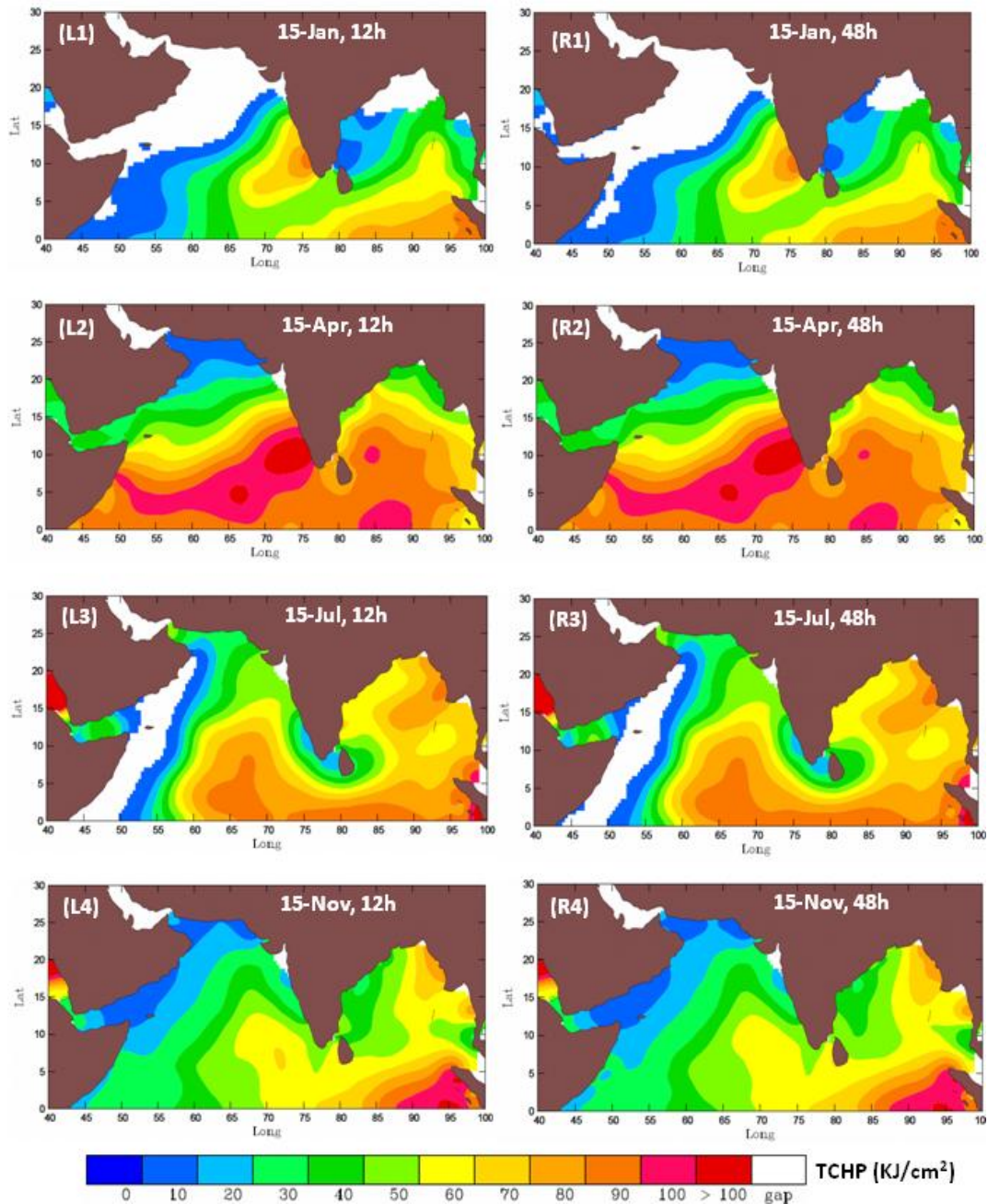


**Figure 11: Spatial Variability of Model Predictions of TCHP on 15<sup>th</sup> day for 4 months during 2012 (L1-L4: 12-h predictions; R1-R4: 48-h predictions)**

## 5. Conclusions

In the present work, an attempt has been made to develop an automated package for prediction of  $D_{26}$  and TCHP 48 hours in advance using a 1-D ocean model. The model is forced with a climatology and AGCM forecasts of meteorological parameters at the ocean surface to provide predictions of  $D_{26}$  and TCHP over the NIO. The model predicted parameters have then been validated by comparison with those obtained from *in situ* Argo observations during the year 2012 for months representative of the four seasons namely, winter monsoon, summer, summer

monsoon and post-summer monsoon periods. Inter-comparisons of the present results and those from Argo observations have also been made with certain other available  $D_{26}$  and TCHP products in the country (results not presented in this report) and the present prediction results have been found to be quite satisfactory and even better in some cases. Following this, the spatio-temporal variability of  $D_{26}$  and TCHP has also been analysed over the NIO during 2012. The entire process starting from data download, pre-processing, model run and visualization integrated into an automated package based on available open source softwares could be used for operational purposes. Regular predictions thus obtained could also be used for ocean monitoring, disaster management and inter-disciplinary academic and applications research.

### **Acknowledgements**

Sincere thanks are due to Director (NRSC), Deputy Director (ECSA, NRSC) & Programme Director (NICES, NRSC), and Group Head (OSG/ECSA, NRSC) for facilitating this work. Sincere thanks are due to all the colleagues of Ocean Sciences Group and Bhuvan team for their sincere support and encouragement. The Argo data used in this work are provided freely under the International Argo Program, hosted by INCOIS through their website. Surface atmospheric forcings from T574 AGCM have been provided by NCMRWF. These institutions/organizations and the national and international programmes contributing to them in making very useful data (WOA05 Climatological T/S profiles, COADS climatology, ETOPO2 bathymetry, Argo and T574) freely available through their web resources, are also gratefully acknowledged.

Sincere thanks are also due to Prof. R. A. Weller of the Woods Hole Oceanographic Institution (WHOI), Woods Hole, Massachusetts, USA for providing the original PWP model code. All the processing, development and visualization tools used in the work are based on freewares/open source softwares. NCAR Command Language (NCL) tools have been used for certain data analysis and visualizations in this work [NCL, 2013].

Part of this work has formed the M. Tech. dissertation thesis for Mr. Navaneeth Krishnan, CUSAT, Kochi.

## References

- Ali, M. M. P. S. V. Jagadeesh, I. I. Lin and Je-. Y. Hsu (2012), A neural network approach to estimate tropical cyclone heat potential in the Indian Ocean, *IEEE – Geosci. Remote Sens. Lett.*, DOI No: 10.1109/LGRS.2012.2191763.
- Ali, M. M., D. Swain, and R. A. Weller (2004), Estimation of ocean subsurface thermal structure from surface parameters: A neural network approach, *Geophys. Res. Lett.*, 31, L20308.
- Ali, M. M., P. S. V. Jagadeesh and S. Jain (2007), Effects of Eddies and Dynamic Topography on the Bay of Bengal Cyclone Intensity, *EOS Trans., AGU*, 88, 93-95.
- Antonov, J. I., R. A. Locarnini, T. P. Boyer, A. V. Mishonov and H. E. Garcia (2006), *World Ocean Atlas 2005, vol 2: Salinity*, S. Levitus (Ed.), NOAA Atlas NESDIS 62, U.S. Govt. Printing Office, Washington D.C., pp. 182.
- Babu, S. V., A. D. Rao and D. K. Mahapatra (2008), “Pre-monsoon variability of Ocean processes along the East Coast of India, *J. Coastal Res.*, 24 (3), 628-639.
- Belanger, J. I., P. J. Webster, J. A. Curry and M. T. Jelinek (2012), Extended prediction of North Indian Ocean tropical cyclones, *Wea. Forecasting*, 27, 757-769.
- Bruce, J. G. (1983), The wind field in the western Indian Ocean related ocean circulation, *Mon. Wea. Rev.*, 111, 1442–1453.
- DeMaria, M. (2009), A simplified dynamical system for tropical cyclone intensity prediction, *Mon. Wea. Rev.*, 137, 68-82.
- DeMaria, M. and J. Kaplan (1994), Sea surface temperature and the maximum intensity of tropical cyclones, *J. Climate*, 7, 1324-1334.
- DeMaria, M., M. Mainelli, L.K. Shay, J.A. Knaff and J. Kaplan (2005), Further improvements to the Statistical Hurricane Intensity Prediction Scheme (SHIPS), *Wea. Forecasting*, 20, 531-543.
- Düing, W. and A. Leetmaa (1980), Arabian Sea cooling, a preliminary heat budget, *J. Phys. Oceanogr.*, 10, 307–312.
- ETOPO2v2 (2006), 2-minute Gridded Global Relief Data, U.S. Dept. Of Commerce, National Oceanic and Atmospheric Administration, National Geophysical Data Center, USA, 2006.
- Goni, G. J. and J. A. Trinanes (2003), Ocean thermal structure monitoring could aid in the intensity forecast of tropical cyclones, *Eos. Trans., AGU*, 84 (51), 573.
- Goni, G. J., M. DeMaria, J. Knaff, C. Sampson, I. Ginis, F. Bringas, A. Mavume, C. Lauer, I. I. Lin, M. M. Ali, P. Sandery, S. Ramos-Buarque, K. Kang, A. Mehra, E. Chassignet and G. Hallowel (2009), Applications of satellite-derived ocean measurements to tropical cyclone intensity forecasting, *Oceanogr.*, 22 (3), 176-183.
- Goni, G. J., S. Kalmholz, S. Garzoli and D. Olson (1996), Dynamics of the Brazil-Malvinas Confluence Based on Inverted Echo Sounders and Altimetry, *J. Geophys. Res.*, 101, 16273-16289.

- Hacker, P., E. Firing, J. Hummon, A. L. Gordon and J. C. Kindle (1998), Bay of Bengal currents during the Northeast Monsoon, *Geophys. Res. Lett.*, 25 (15), 2769-2772.
- Hastenrath, S. (1980), Heat Budget of Tropical Ocean and Atmosphere, *J. Phys. Oceanogr.*, 10, 159-170.
- Jaswal, A. K., V. Singh and S. R. Bhambak (2012), Relationship between sea surface temperature and surface air temperature over Arabian Sea, Bay of Bengal and Indian Ocean, *J. Ind. Geophys. Union*, 16 (2), 41-53.
- Kumar, S. P. and T. G. Prasad (1996), Winter cooling in the northern Arabian Sea, *Curr. Sci.*, 71, 834-841.
- Kumar, S. P. and J. Narvekar (2005), Seasonal variability of the mixed layer in the central Arabian Sea and its implication on nutrients and primary productivity, *Deep Sea Res. - 2*, 52 (14-15), 1848-1861.
- Kumar, S. P. and J. Narvekar (2006), Seasonal variability of the mixed layer in the central Bay of Bengal and associated changes in nutrients and chlorophyll, *Deep Sea Res. - 1*, 53 (5), 820-835.
- Locarnini, R. A., A. V. Mishonov, J. I. Antonov, T. P. Boyer and H. E. Garcia (2006), *World Ocean Atlas 2005, vol 1: Temperature*, S. Levitus (Ed.) NOAA Atlas NESDIS 61, U.S. Govt. Printing Office, Washington D.C., pp. 182.
- Millero, F. J. and A. Poisson (1981), International one-atmosphere equation of state of seawater, *Deep Sea Research - A*, 28 (6), 625 – 629.
- Mohan, K. and A. K. Gupta (2011), Intense deep convective mixing in the southeast Arabian Sea linked to strengthening of the northeast Indian monsoon during the middle Pliocene, *Curr. Sci.*, 101 (4), 543.
- Momin, I. M., R. Sharma and S. Basu (2011), Satellite derived heat content in the tropical Indian Ocean, *Remo. Sens. Lett.*, 2, 269-277.
- Mowla, K. G. (1970), Cyclogenesis in the Bay of Bengal and the Arabian Sea, *Tellus*, 22 (6), 716-718.
- Muraleedharan, P. M. and S. P. Kumar (1996), Arabian Sea Upwelling- A comparison between coastal and open ocean regions, *Curr. Sci.*, 71, 842-846.
- Murtugudde, R. and A. J. Busalacchi (1999), Interannual variability of the dynamics and thermodynamics, and mixed layer processes in the Indian Ocean, *J. Climate*, 12, 2300–2326.
- NCL (2013), The NCAR Command Language (Version 6.1.1) [Software], Boulder, Colorado: UCAR/NCAR/CISL/VETS, <http://dx.doi.org/10.5065/D6WD3XH5>.
- Panchawagh, N. V. (2006), Seasonal variation of SST and mean OLR distribution over Indian Ocean Warmpool, *J. Ind. Geophys. Union*, 10 (3), 167-173.

- Potemra, J. T., M. E. Luther and J. J. O'Brien (1991), The seasonal circulation of the upper ocean in the Bay of Bengal, *J. Geophys. Res.*, 96, 12 667–11 683.
- Prasad, T. G. (1997), Annual and seasonal mean buoyancy fluxes for the tropical Indian Ocean, *Curr. Sci.*, 73, 667–674.
- Price, J. F., R. A. Weller and R. Pinkel (1986), Diurnal cycling: Observations and models of the upper ocean response to diurnal heating, cooling and mixing, *J. Geophys. Res.*, 91(C7), 8411-8427.
- Rao, D. S., C. P. Ramamirtham, A. V. S. Murthy, S. Muthusamy, N. P. Kunhikrishnan and L. R. Khambadkar (1992), Oceanography of the Arabian Sea with particular reference to the southwest monsoon, *CMFRI Bulletin*, 45, 4-8.
- Shankar, D., J. P. McCreary, W. Han and S. R. Shetye (1996), Dynamics of the East India Coastal Current 1. Analytical solutions forced by interior Ekman pumping and local alongshore winds, *J. Geophys. Res.*, 101, 13 975–13 991.
- Shay, L. K. G. J. Goni, and P. G. Black (2000), Effects of a warm oceanic feature on Hurricane Opal, *Mon. Wea. Rev.*, 128, 1366-1383.
- Shetye, S. R., A. D. Gouveia, D. Shankar, S. S. C. Shenoi, P. N. Vinayachandran, D. Sunder, G. S. Michael and G. Nampoothiri (1996), Hydrography and circulation in the western Bay of Bengal during the Northeast monsoon, *J. Geophys. Res.*, 101, 14 011–14 025.
- Suryanarayana, A., V. S. N. Murthy, Y. V. B. Sarma, M. T. Babu, D. P. Rao and J. S. Sastry (1992), Hydrographic features of the western Bay of Bengal in the upper 500 m under the influence of NE and SW monsoon, *Oceanogr. Ind. Ocean*, 595-604.
- Swain, D. and M. M. Ali (2011), One-dimensional Price-Weller-Pinkel model for mixed layer depth predictions, *NRSC Technical Report ver. 1.0*, NRSC: RS&GISAA:ESAG:OD:DEC11:TR365, ISRO, pp: 25.
- Swallow, J. C. (1984), Some aspects of the physical oceanography of the Indian Ocean, Institute of Oceanography Sciences (NERC), Surrey, UK, 31(6-8), 639-650.
- Takeshi, I., C. B. Montegut, J-J. Luo, S. K. Behera, S. Masson and T. Yamagata (2008), The Role of Western Arabian Sea Upwelling in Indian Monsoon Rainfall Variability, *J. Climate*, 21 (21), 5603-5623.
- Varkey, M. J., V. S. N. Murty and A. Suryanarayana (1996), Physical Oceanography of the Bay of Bengal and Andaman Sea, *Oceanogr. Mar. Bio.: An Ann. Rev.*, 34, 1–70.
- Vinayachandran, P. N. (2004), Summer cooling of the Arabian Sea during contrasting monsoons, *Geophys. Res. Lett.*, 31, L13306, doi:10.1029/2004GL019961.
- Vinayachandran, P. N. and S. R. Shetye (1991), The warm pool in the Indian Ocean, *Procee. Ind. Acad. Sci- Earth and Planetary Sciences*, 100 (2), 165-175.
- Wada, A., and J. C. L. Chan (2008), Relationship between typhoon activity and upper ocean heat content, *Geophys. Res. Lett.*, 35, L17603.

- Wada, A., and N. Usui (2007), Importance of tropical cyclone heat potential for tropical cyclone intensity and intensification in the Western North Pacific, *J. Oceanogr.*, 63, 427-447.
- Webster, P. J., V. O. Magana, T. N. Palmer, J. Shukla, R. T. Tomas, M. Yanai and T. Yasunari (1998), Monsoons: Processes, predictability and the prospects of prediction, *J. Geophys. Res.*, 103, 14 451–14 510.
- WMO/TD No. 84 (2011), Tropical cyclone operationa; plan for the Bay of Bengal and the Arabian Sea, *Tropical Cyclone Programme Report No. TCP-21*, 2011, pp: 103.

## Appendix – I

### Package Execution Environment

(a) Hardwares:

- (i) Standard PC (Tested on Workstation and Server Environment)
- (ii) Disk Space: 10 GB (initially) with ~ 500 MB serving as flash
- (ii) RAM: 1 GB or higher

(a) OS/Compilers

- (i) Linux/Unix (Tested on Ubuntu 9.04 & 10.04, RedHat ver 5.0; 32 & 64 bit machines)
- (ii) NCL Libraries
- (iii) NetCdf Libraries
- (iv) Fortran Compiler (Tested with ifort & f90)
- (v) Linux Scheduler (Crontab) setting or equivalent
- (vi) Internet and ftp Access

(b) Visualization Packages

- (i) NCAR-Graphics/MATLAB/Grads (Tested on NCAR-Graphics)

## Appendix – II

### Locations of ARGO floats used for validation of model results

Sl. No.	Latitude (°N)	Longitude (°E)	Sl. No.	Latitude (°N)	Longitude (°E)
1	1.06	77.50	28	13.01	86.19
2	1.50	55.50	29	13.22	67.29
3	2.50	92.50	30	13.44	49.71
4	2.81	69.09	31	13.50	67.00
5	3.27	65.54	32	14.50	55.50
6	3.74	93.71	33	14.69	59.43
7	4.00	49.50	34	14.70	88.06
8	4.64	89.17	35	14.74	56.99
9	4.78	62.02	36	15.14	67.15
10	4.89	64.71	37	15.83	91.42
11	7.00	53.50	38	15.85	89.86
12	8.00	85.50	39	15.99	92.26
13	8.47	84.66	40	16.19	58.03
14	9.19	88.22	41	16.26	87.28
15	9.45	82.42	42	16.92	85.68
16	9.47	87.67	43	16.99	88.88
17	9.50	87.00	44	17.00	89.00
18	10.22	70.66	45	17.75	67.86
19	10.47	88.06	46	17.79	92.19
20	10.68	85.19	47	17.93	59.97
21	11.00	85.50	48	18.08	92.68
22	11.50	86.50	49	18.48	65.52
23	11.87	70.28	50	20.75	65.25
24	12.07	85.98	51	22.50	62.50
25	12.41	83.67	52	23.79	64.72
26	12.67	86.29	53	23.79	64.72
27	12.73	57.26	54	23.79	64.72



NRSC-ECSA-OSG-May2013-TR-529

*Ocean Sciences Group  
(Earth & Climate Science Area)  
National Remote Sensing Centre  
ISRO (Govt. of India, Dept. of Space)  
Balanagar, Hyderabad-500037, INDIA*

